Lotus japonicus symbiosis genes impact microbial interactions between symbionts and multikingdom commensal communities

Thorsten Thiergart [§ 1,2], Rafal Zgadzaj [§ 1], Zoltán Bozsóki [3], Ruben Garrido-Oter [1,2], Simona Radutoiu[*3], and Paul Schulze-Lefert[*1,2]

[1]Max Planck Institute for Plant Breeding Research, 50829 Cologne, Germany.

[2]Cluster of Excellence on Plant Sciences (CEPLAS), Max Planck Institute for Plant Breeding Research, 50829 Cologne, Germany.

[3]Department of Molecular Biology and Genetics, Faculty of Science and Technology, Aarhus University, 8000 C Aarhus, Denmark.

§ joint first authors

* co-corresponding authors, (radutoiu@mbg.au.dk , S.R., schlef@mpipz.mpg.de , P.S.-L.)

Abstract

The legume *Lotus japonicus* engages in mutualistic symbiotic relationships with arbuscular mycorrhiza (AM) fungi and nitrogen-fixing rhizobia. Using plants grown in natural soil and community profiling of bacterial 16S *rRNA* genes and fungal internal transcribed spacers (ITS), we examined the role of the *Lotus* symbiosis genes *RAM1*, *NFR5*, *SYMRK*, and *CCaMK* in structuring bacterial and fungal root-associated communities. We found host genotype-dependent community shifts in the root and rhizosphere compartments that were confined to bacteria in *nfr5* or fungi in *ram1* mutants, whilst *symrk* and *ccamk* plants displayed changes across both microbial kingdoms. We observed in all AM mutant roots an almost complete depletion of Glomeromycota taxa that was accompanied by a concomitant enrichment of Helotiales and Nectriaceae fungi, suggesting compensatory niche replacement within the fungal community. A subset of Glomeromycota whose colonization is strictly dependent on the common symbiosis pathway was retained in *ram1* mutants, indicating that *RAM1* is dispensable for intraradical colonization by some Glomeromycoyta fungi. However, intraradical colonization by bacteria belonging to the Burkholderiaceae and Anaeroplasmataceae is dependent on AM root infection, revealing a microbial interkingdom interaction. Despite an overall robustness of the bacterial root microbiota against changes in the composition of root-associated fungal assemblages, bacterial and fungal co-occurrence network analysis demonstrates that simultaneous disruption of AM and rhizobia symbiosis increases the connectivity among taxa of the bacterial root microbiota. Our findings imply a broad role for *Lotus* symbiosis genes in structuring the root microbiota and identify unexpected microbial interkingdom interactions between root symbionts and commensal communities.

Importance

Studies on symbiosis genes in plants typically focus on binary interactions between roots and soil-borne nitrogen-fixing rhizobia or mycorrhizal fungi in laboratory environments. We utilized wild-type and symbiosis mutants of a model legume, grown in natural soil, in which the bacterial or fungal or both symbioses are impaired to examine potential interactions between the symbionts and commensal microorganisms of the root microbiota when grown in natural soil. This revealed microbial interkingdom interactions between the root symbionts and fungal as well as bacterial commensal communities. Nevertheless, the bacterial root microbiota remains largely robust when the fungal symbiosis is impaired. Our work implies a broad role for host symbiosis genes in structuring the root microbiota of legumes.

Introduction

Mutualistic plant-microbe interactions are essential adaptive responses dating back to plant colonization of terrestrial habitats [1,2]. Endosymbiotic association with obligate arbuscular mycorrhizal (AM) fungi belonging to the phylum Glomeromycota is considered to have enabled early land plants to adapt to and survive harsh edaphic conditions by improving the acquisition of nutrients, especially phosphorus, from soil [3]. It is estimated that approximately 80% of extant plant species remain proficient in AM symbiosis (AMS), testifying to its importance for survival in natural ecosystems [4,5,6]. Another more recent endosymbiotic relationship has evolved between plants belonging to distinct lineages of flowering plants (Fabales, Fagales, Cucurbitales, and Rosales) and nitrogen-fixing members of the Burkholderiales, Rhizobiales or Actinomycetales, enabling survival on nitrogen-poor soils. These bacteria fix atmospheric nitrogen under the low oxygen conditions that are provided by plant root nodules.

Studies using mutant legumes deficient in both AM and root nodule symbiosis (RNS) revealed that a set of genes defined as the common symbiotic signaling pathway (CSSP) are crucial for these symbioses. In the model legume *Lotus japonicus*, Nod factor perception by NFR1 and NFR5 activates downstream signaling through SYMRK, a malectin and leucine-rich repeat (LRR)-containing receptor-like kinase (RLK) [7], currently considered to be the first component of the CSSP. SYMRK associates with NFR5 through a mechanism involving intramolecular cleavage of the SYMRK ectodomain, thereby exposing its LRR domains [8]. Signaling from the plasma membrane is transduced to the nuclear envelope where ion channels [9,10], nuclear pore proteins [11,12,13] and cyclic nucleotide-gated channels [14] mediate symbiotic calcium oscillations. These

calcium oscillations are interpreted by the calcium- and calmodulin-dependent protein kinase CCaMK, [15,16] that interacts with the DNA binding transcriptional activator CYCLOPS [17,18,19]. Several GRAS transcription factors (NSP1, NSP2, RAM1, RAD1) are activated downstream of CCaMK and CYCLOPS and determine whether plants engage in AMS or RNS symbiosis.

Plants establish symbioses with AM fungi and nitrogen-fixing bacteria by selecting interacting partners from the taxonomically diverse soil biome. These interactions are driven by low mineral nutrient availability in soil and induce major changes in host and microbial symbiont metabolism [20,21]. Although RNS develops as localized events on legume roots, analysis of *Lotus* mutants impaired in their ability to engage in symbiosis with nitrogen-fixing bacteria revealed that these mutations do not only abrogate RNS, but also impact the composition of taxonomically diverse root- and rhizosphere-associated bacterial communities, indicating an effect on multiple bacterial taxa that actively associate with the legume host, irrespective of their symbiotic capacity [22]. By contrast, the effect of AMS is known to extend outside the host *via* a hyphal network that can penetrate the surrounding soil and even indirectly affect adjacent plants [23]. In soil, fungal hyphae themselves represent environmental niches and are populated by a specific set of microbes [24]. Although the biology of AMF is well understood and genetic disruption of AMS was recently shown to exert a relatively small effect on root-associated fungal communities in *Lotus* [25], the potential impact of AMS and/or RNS on root-associated bacterial and fungal commensals remains poorly understood, mainly because previous studies have their focus on either bacteria [22] or fungi alone [25].

We reasoned that the model legume *Lotus japonicus,* with its well-characterized symbiosis signaling mutants impaired in RNS, AMS, or both is particularly useful to examine whether genetic perturbations of these symbioses impact only commensal communities of the corresponding microbial kingdom and/or influence microbial interkingdom interactions in the root microbiota. We applied bacterial and fungal community profiling experiments to root samples collected from wild-type (WT) *L. japonicus* and four symbiosis signaling mutants, grown in natural soil. We show that genetic disruption of the symbioses results in significant host genotype-dependent microbial community shifts in the root and surrounding rhizosphere compartments. These changes were mainly confined to either bacterial or fungal communities in RNS- or AMS-deficient plant lines, respectively, whereas mutants with defects in the CSPP revealed major changes in assemblages of the root microbiota across both microbial kingdoms. We found that perturbation of AM symbiosis alone is sufficient to deplete a subset of bacterial taxa belonging to the Burkholderiaceae and

107 Anaeroplasmataceae families from the root microbial community, whereas simultaneous
108 perturbation of AM and rhizobia symbioses increases the connectivity within the bacterial root co-
109 occurrence network.

110 **Results**

111 **Root fractionation protocol affects the composition of associated bacterial communities**

112 Earlier physiological studies have shown that only cells of a specific developmental stage, located
113 in the root elongation zone, respond to Myc and Nod factors, mount symbiotic calcium oscillations
114 and enable epidermal infection by rhizosphere-derived fungal and bacterial symbionts [26,27]. To
115 explore spatial organization of root-associated bacterial and fungal communities along the
116 longitudinal axis, we collected samples of the upper and lower root zones as well as the entire root
117 system of 10 week-old Gifu wild-type plants, grown in Cologne soil (2 to 5 cm and >9 cm of the root
118 system, respectively; Fig. 1A; [28]). Microbial assemblages of these three root endosphere
119 compartments were compared to the communities in the corresponding rhizosphere fractions, i.e.
120 soil tightly adhering to the respective root zones, and with the bacterial biome present in unplanted
121 Cologne soil. 16S rRNA gene amplicon libraries of the V5-V7 hypervariable region and gene
122 libraries of the Internally Transcribed Spacer 2 (ITS2) region of the eukaryotic ribosome were
123 generated by amplification [29,30,31]. Information on the number and relative abundance of
124 operational taxonomic units (OTUs) in each compartment was used to calculate α– (Shannon
125 index; within sample diversity) and β-diversity (Bray-Curtis distances; between samples diversity),
126 OTU enrichment and taxonomic composition. In bacteria we observed a gradual decrease in α-
127 diversity from unplanted soil to the rhizosphere and to the root endosphere compartments, a trend
128 that was similar for each longitudinal root fraction. This suggests that winnowing of root
129 commensals from the highly complex soil biome occurs in all tested root zones (Fig. S1A). Similar
130 overall results were obtained for the fungal dataset (Fig. S1B), but the decrease in diversity from
131 unplanted soil towards the rhizosphere was mild or even lacking. The latter finding is similar to that
132 of a recent study of root-associated fungi in non-mycorrhizal *A. thaliana* sampled at three natural
133 sites [32]. Analyses of taxonomic composition and β-diversity revealed striking differences in the
134 endosphere and rhizosphere compartments associated with the upper and lower root longitudinal
135 fractions. The composition of bacterial and fungal taxa of the whole root closely resembled that of
136 the upper root fraction (Fig. 1B), with only low numbers of OTUs differentially abundant between
137 these two compartments (Fig. 1C and 1D). This suggests that microbes colonizing the lower root
138 fraction constitute only a small fraction of the entire *Lotus* root microbiota. Additionally, we

139 observed a higher sample-to-sample variation in the taxonomic profiles of the lower root zone
140 compared to the upper whole root fractions (Fig. 1B). This greater community variation in the
141 developmentally younger region of *L. japonicus* roots might reflect a nascent root microbiota or
142 greater variation in root tissue and adherent rhizosphere samples that we recovered from this root
143 zone by our fractionation protocol. Based on the finding that whole root and upper root
144 compartments host comparable bacterial communities and given their greater stability we decided
145 to use the former for further analyses.

146 **Host genes needed for symbioses determine bacterial and fungal community composition**
147 **of *L. japonicus* root and rhizosphere**

148 For root microbiota analysis, we cultivated wild-type (ecotype Gifu) *L. japonicus* and *nfr5-2*, *symrk-*
149 *3*, *ccamk-13* and *ram1-2 (nfr5, symrk, ccamk* and *ram1,* from thereof*)* mutant genotypes in parallel
150 in two batches of Cologne soil, to account for batch-to-batch and seasonal variation at the
151 sampling site. *nfr5-2* mutant plants are impaired in rhizobial Nod factor perception and signaling,
152 which prevents initiation of infection thread formation [33]. Mutations in *SymRK* and *CCaMK* affect
153 the common symbiosis pathway downstream of Nod or Myc factor perception, abrogating infection
154 either by nitrogen fixing rhizobia or AM fungi [7,34]. The RAM1 transcription factor controls
155 arbuscule formation, and while *ram1* mutants of *L. japonicus* are indistinguishable from wild type
156 and permit incipient AM fungus infection, fungal colonization is terminated with the formation of
157 stunted symbiotic structures [35]. All plant genotypes appeared healthy (Fig. 2A-E), but the shoot
158 length and shoot fresh weight of all mutant plants was significantly reduced in comparison to wild
159 type (Fig. 2F and 2G), suggesting that genetic disruption of either AM or *Rhizobium* symbiosis is
160 detrimental for the fitness of plants grown in natural soil. All genetic defects in nitrogen-fixing
161 symbiosis, validated by the absence of root nodules in *nfr5*, *symrk* and *ccamk* genotypes (Fig. 2C-
162 E, Table S1), resulted in similarly severe impacts on plant growth (Fig. 2F and 2G), whereas both
163 shoot length and shoot fresh weight were significantly but less severely reduced in *ram1* plants.
164 *ram1* plants still formed nodules and, unlike WT and *nfr5*, showed impairment in AM symbiosis
165 (Table S1).

166 In order to determine the impact of rhizobial and AM symbiosis on root microbiota assembly, we
167 characterized fungal and bacterial communities of unplanted Cologne soil, rhizosphere, and root
168 compartments of all aforementioned *L. japonicus* genotypes at bolting stage. Visible nodules and
169 root primordia were removed from the roots of nodulating wild type and *ram1* genotypes prior to
170 sample processing for community profiling. We amplified the V5-V7 hypervariable region of the

171 bacterial 16S rRNA gene and the ITS2 region of the eukaryotic ribosomal genes. High-throughput
172 sequencing of these amplicons yielded 22,761,657 16S and 21,228,781 ITS reads, distributed in
173 222 and 274 samples, respectively, which were classified into 5,780 and 3,361 distinct microbial
174 OTUs. Analysis of α-diversity revealed a general reduction of complexity from unplanted soil to
175 rhizosphere and lastly to root compartments for bacterial communities, whereas the complexity of
176 fungal communities was similar for the plant-associated compartments (Fig. S2A and S2B), which
177 is consistent with a recent study of *A. thaliana* root-associated fungal communities [32]. Bacterial
178 α-diversity was slightly elevated in the *nfr5* genotype in rhizosphere and root compartments in
179 comparison to all other genotypes (Fig. S2A). Fungal communities were similarly diverse in the
180 rhizosphere of all tested plant genotypes, but their diversity in the root compartment was
181 significantly and specifically reduced in all three AM mutants (*ccamk*, *ram1*, and *symrk*; Fig. S2B).

182 Analysis of β-diversity using Principal Coordinate Analysis (PCoA) of Bray-Curtis distances
183 showed a significant effect of soil batch on soil-resident bacterial and fungal communities (Fig. S2C
184 and D). In order to account for this technical factor and assess the impact of the different host
185 compartment and genotypes in community composition, we performed a Canonical Analysis of
186 Principle Components Coordinates (CAP; [36]). This revealed a clear differentiation of bacterial
187 and fungal communities in the tested plant genotypes in both root and rhizosphere compartments,
188 with the host genotype explaining as much as 7.61% of the overall variance of the 16S rRNA, and
189 13.5% of ITS2 data (Fig. 3; $P<0.001$). The rhizosphere compartments of wild type and *ram1* were
190 found to harbor similar bacterial communities, but were separate from those of *symrk* and *ccamk*
191 (Fig. 3A). Further, the rhizosphere communities of each of these four plant genotypes were found
192 to be significantly different from that of *nfr5* (Fig. 3A). A similar trend was observed for fungal
193 communities, except that wild-type and *ram1* rhizosphere communities were clearly separated from
194 each other (Fig. 3C). In the root compartment we found bacterial consortia that were distinctive for
195 each of the five plant genotypes (Fig. 3B). This genotype effect was also found in the root-
196 associated fungal communities, with the exception of *nfr5*, which was indistinguishable from wild-
197 type (Fig. 3D). We then tested the contribution of AM and rhizobial symbionts to the observed
198 patterns of diversity, in order to determine if AM fungi (Glomeromycota) and nitrogen-fixing
199 *Mesorhizobium loti* (Phylobacteriaceae) are the sole drivers of these host genotype community
200 shifts (Fig. 3). We performed an *in silico* experiment in which sequencing reads of these two
201 symbiotic taxonomic groups were removed from the analyses. Although we observed a decrease
202 in the percentage of variance explained by the host genotype (Fig. S3 compared to Fig. 3), overall
203 patterns of β-diversity remained unaltered, suggesting that other community members besides root

204 nodule and arbuscular mycorrhizal symbionts contribute to the plant genotype-specific community
205 shifts. Collectively, our analyses of *L. japonicus* symbiotic mutants grown in natural soil show that
206 lack of AM and/or RNS symbioses has a significant effect on plant growth and on the structures of
207 bacterial and fungal communities associated with legume roots.

208 **Loss of symbiosis affects specific bacterial and fungal families of the root microbiota**

209 Comparison of bacterial family abundances between wild type and mutants lacking RNS and/or
210 AM symbiosis identified significant changes in Comamonadaceae, Phyllobacteriaceae,
211 Methylophilaceae, Cytophagaceae and Sinobacteraceae in the rhizosphere compartment (Fig. 4A;
212 top 10 most abundant families). The abundance of Comamonadaceae and Phyllobacteriaceae also
213 differed significantly in the root compartment of RNS mutants compared to wild type.
214 Streptomycetaceae and Sinobacteraceae were specifically affected by loss of *Nfr5*, whereas
215 Anaeroplasmataceae and Burkholderiaceae were affected by the lack of AM symbiosis in *symrk*
216 and *ccamk* plants (Fig. 4A). The relative abundances of the same two families were also
217 significantly reduced in *ram1* roots, suggesting that active AM symbiosis influences root
218 colonization by a subset of bacterial root microbiota taxa. Six out of the ten most abundant fungal
219 families in the rhizosphere compartment of *Lotus* plants belonged to Ascomycota (Fig. 4B). By
220 contrast, the root endosphere was dominated by numerous families of Glomeromycota, which were
221 found to be almost fully depleted from the rhizosphere and root compartments of *ram1*, *symrk* and
222 *ccamk* mutants, indicating that absence of AM symbiosis predominantly affects Glomeromycota
223 and does not limit root colonization or rhizosphere association by other fungal families. However,
224 depletion of Glomeromycota in the AM mutant roots was accompanied by an increase in the
225 relative abundance of Ascomycota members belonging to Nectriaceae in both rhizosphere and root
226 compartments and by an increased abundance of unclassified Helotiales, Leotiomycetes, and
227 Sordariomycetes in the root compartment only (Fig. 4B).

228 Closer inspection of the microbial community shifts at the OTU level identified 45 bacterial OTUs
229 and 87 fungal OTUs enriched in the roots of symbiosis mutants compared to those of wild type
230 (Fig. 5), and 60 bacterial OTUs and 30 differentially abundant fungal OTUs in the rhizosphere
231 samples (Fig. S4). The absence of RNS in *nfr5* roots affected the relative abundance of multiple
232 OTUs (n=27 in the root, n=23 in the rhizosphere) belonging to diverse taxa. Many of these OTUs
233 (n=18 in the root, n=16 in the rhizosphere) showed a similar differential relative abundance in
234 *symrk* and/or *ccamk* mutants when compared to wild type (Fig.5A), indicating that their contribution
235 to the *Lotus* root communities outside of nodules is affected by active nitrogen fixing symbiosis.

236 Impairment of both AM and RNS symbioses in *symrk* and/or *ccamk* mutants resulted in opposite
237 changes in the relative root abundances of OTUs belonging to specific Burkholderiales families.
238 Depletion of OTUs belonging to Burkholderiaceae (n=5) was accompanied by the enrichment of
239 OTUs from other Burkholderiales families (Oxalobacteraceae [n=3], Comamonadadaceae [n=2],
240 and Methylophilaceae [n=2]; Fig. 5A). Only three of the above-mentioned Burkholderiaceae OTUs
241 were depleted in *ram1* roots, suggesting that their enrichment in *Lotus* roots is dependent on
242 functional AM symbiosis.

243 Analysis of the ITS2 amplicon sequences from root samples identified a large number of
244 Glomeromycota OTUs (n=39), demonstrating the capacity of *Lotus* Gifu roots grown in natural soil
245 to accommodate a phylogenetically diverse community of AM fungi (Fig. 5B). The majority of these
246 fungal OTUs (n=31) were depleted in *symrk*, *ccamk* and *ram1* mutant roots, indicating that their
247 enrichment is dependent on a functional AM symbiosis pathway. Their intraradical colonization
248 appears to be independent of *RAM1*, as 12 OTUs assigned to Glomeromycota or unclassified, nine
249 of which define a Glomeromycota sublineage, were depleted in *symrk* and *ccamk* but not in *ram1*
250 roots. A reduced abundance of Glomeromycota OTUs in the endosphere compartment was
251 accompanied by an increased abundance of Ascomycota members, especially of members
252 belonging to the Nectriaceae (8 OTUs) and Helotiales (7 OTUs) families, suggestive of a mutually
253 exclusive occupancy of the intraradical niche. In sum, our results reveal that in natural soil CSSP
254 symbiotic genes are essential for root colonization by a wide range of Glomeromycota fungi and
255 that these genes significantly affect the abundances of multiple bacterial taxa, predominantly
256 belonging to the Burkholderiales and Rhizobiales orders.

257 In order to assess the impact of mutations of *Lotus* symbiotic genes on microbial interactions we
258 constructed co-occurrence microbial networks for each genotype independently using SparCC [37]
259 (Fig. S5). We observed an increase in the number of edges of the networks inferred from *symrk*
260 and *ccamk* (748 and 805 edges, respectively) compared to Gifu WT, *nfr5*, and *ram1* networks
261 (471, 569 and 500 edges, respectively; Fig S5 A), despite a comparable number of nodes in all
262 genotypes. This unexpected observation suggests a greater connectivity between bacterial root
263 commensals when both fungal and bacterial symbioses are disrupted in *symrk* and *ccamk* roots. In
264 the corresponding five fungal networks the number of OTUs is moderately reduced in *ram1* and
265 approximately halved in *symrk* and *ccamk* networks (86 in Gifu WT*,* 78 in *nfr5,* 63 in *ram1*, 39 in
266 *symrk*, 41 in *ccamk*; Fig S5 A), which can be explained by the partial or complete depletion of
267 Glomeromycota taxa in the latter three host genotypes. This decrease in the number of fungal

268 OTUs is accompanied by a decrease in the number of edges in the fungal networks (329 Gifu, 363
269 *nfr5*, 231 *ram1*, 101 *symrk* and 117 edges in *ccamk*, respectively; Fig S5 A). To directly compare
270 the number of edges between plant genotypes for bacterial and fungal networks we first
271 normalized the number of bacterial and fungal OTUs (Fig S5 B). Compared to Gifu WT and *nfr5*
272 networks the degree centrality for bacterial OTUs is slightly increased in *ram1* (significant only for
273 positive correlations) and clearly increased in *symrk* and *ccamk* (significant for both positive and
274 negative correlations), supporting the aforementioned change in network structure of the bacterial
275 root microbiota when both fungal and bacterial symbiosis are disrupted in *Lotus* roots. By contrast,
276 the degree centrality of fungal OTUs remains mostly stable across fungal networks identified in the
277 five plant genotypes. Together our analyses suggest that the combined activities of fungal and
278 bacterial symbioses negatively influence the connectivity within the *Lotus* bacterial root microbiota.

279 **Discussion**

280 Here we investigated the role of host AM and/or RNS genes in establishing structured bacterial and
281 fungal communities in the rhizosphere and endosphere compartments of *L. japonicus* grown in
282 natural soil. Impairment of RNS in *nfr5* or AMS in *ram1* plants had a significant impact on root
283 microbiota structure, which was mainly, but not exclusively, confined to the composition of
284 corresponding bacterial or fungal communities, respectively (Fig. 3, 4, and 5).

285 The shift between the root-associated microbial communities of wild type and *nfr5-2* mutant is in
286 line with both the qualitative and quantitative findings of a previous report on the *Lotus* bacterial
287 root microbiota (Fig. 3A and B in this study; [22]). Here, however, we observed an enhanced
288 rhizosphere effect in both wild type and *nfr5* plants, leading also to a less prominent community
289 shift in this compartment (Fig. S6), which was not previously observed. These differences in
290 rhizosphere bacterial composition are likely caused by a soil batch effect and, to a lesser extent,
291 possibly also the use of different sequencing platforms (Illumina in this study *versus* 454
292 pyrosequencing in [22]). The nearly unaltered fungal community composition in *nfr5* mutant plants
293 compared to wild type (only 3 out of 39 Glomeromycota OTUs differentially abundant) suggests
294 that NFR5 is dispensable for fungal colonization of *L. japonicus* roots. This is consistent with recent
295 findings from analyses of diverse AM symbiotic mutants of *Lotus* where the structure of the root-
296 associated fungal communities of AM- and CSSP-deficient mutants was indistinguishable [25].
297 Despite unaltered fungal communities in *nfr5* mutants, we found a marked shoot biomass reduction
298 of this genotype grown in natural soil (~4-fold; Fig. 2), revealing that intraradical colonization by
299 soil-derived fungal endophytes is robust against major differences in plant growth.

300 A recent microbial multi-kingdom interaction study in *A. thaliana* showed that bacterial commensals
301 of the root microbiota are crucial for the growth of a taxonomically wide range of fungal root
302 endophytes. These antagonistic interactions between bacterial and fungal root endophytes are
303 essential for plant survival in natural soil [32]. We have shown here that an almost complete
304 depletion of diverse Glomeromycota taxa from roots of each of the three AM mutants was
305 accompanied by an enrichment of fungal OTUs belonging to the families Nectriaceae and
306 Helotiales (Fig. 4). We speculate that the increased relative abundance of these fungal taxa is
307 caused by intraradical niche replacement as a compensatory effect following the exclusion of
308 Glomeromycota symbionts from the root compartment. Previous mono-association experiments
309 have shown that isolates belonging to Nectriaceae and Helotiales can have either mutualistic or
310 pathogenic phenotypes [38,39,40]. Given that all plant genotypes were free of disease symptoms
311 when grown in natural soil (Fig. 2), we speculate that the complex shifts in the composition of the
312 bacterial root microbiota in *nfr5, symrk,* and *ccamk* mutants did not affect the capacity of bacterial
313 endophytes to prevent pathogenic fungal overgrowth. Of note, Helotiales root endophytes were
314 also enriched in roots of healthy *Arabis alpina*, a non-mycorrhizal plant species and relative of *A.*
315 *thaliana*, and contribute to phosphorus nutrition of the host when grown in extremely phosphorus-
316 impoverished soil [41]. The enrichment of Helotiales in *Lotus* AM mutants is therefore consistent
317 with potential niche replacement by other fungal lineages to ensure plant nutrition in nutrient-
318 impoverished soils. Although the proposed compensatory effect in AM mutants will need further
319 experimental testing in phosphorus-depleted soils, our hypothesis is consistent with the only mild
320 impairment in plant growth in *ram1* mutants (Fig. 2).

321 We observed that members of the bacterial families of Burkholderiaceae and Anaeroplasmataceae
322 are significantly depleted in the roots of each of the three AM mutants compared to wild type.
323 Members of the Glomeromycota have been found to contain intracellular endosymbiotic bacteria
324 [42], some belonging to the order Burkholderiales [41]. Interestingly, the most positively correlated
325 bacterial OTUs with Glomeromycota fungi in our network analyses included one
326 Anaeroplasmataceae and two Burkholderiaceae OTUs (Fig. S7), further indicating a direct
327 interaction between these taxonomic groups. These findings suggest that these bacteria are either
328 endosymbionts of Glomeromycota fungi that are excluded from the roots of the AM defective
329 genotypes or that their intraradical colonization is indirectly mediated by AM fungus infection.
330 Except small changes in the bacterial root microbiota in *ram1* plants, which are mainly limited to
331 the aforementioned Burkholderiaceae and Anaeroplasmataceae OTUs, the structure of the root-
332 associated bacterial community is remarkably robust against major changes in the composition of

333 root-associated fungal assemblages (Fig. 5). Nevertheless, we observed a clear increase in
334 connectivity between bacterial OTUs and degree centrality parameters in the bacterial networks
335 constructed from *symrk* and *ccamk* mutants compared to those of Gifu, *nfr5* and *ram1*. This
336 unexpected change in bacterial network structure could be a consequence of a vacant niche
337 created by depletion of dominant Glomeromycota taxa from the interior of *symrk* and *ccamk* roots.
338 But niche filling by bacterial commensals is unlikely to explain the observed alteration in bacterial
339 network connectivity because Glomeromycota root colonization is greatly diminished in *ram1*
340 plants without major changes in the corresponding bacterial network structure (Fig. 4 and Fig. S5).
341 Increased bacterial network connectivity in *symrk* and *ccamk* roots is more likely a consequence of
342 inactivation of the CSSP, which remains intact in all other tested genotypes. However, we cannot
343 fully exclude that the altered nutritional status in *symrk* and *ccamk* plants resulting from the
344 combined loss of metabolic activities of, and induced by both symbionts also plays a role in the
345 altered network structure.

346 Paleontological and phylogenomic studies established the ancestral origin of genetic signatures
347 enabling AM symbiosis in land plants [1,44]. In monocots and dicots, the extended AM fungal
348 network is primarily recognized as a provider of nutrients, particularly phosphorus [45,46], but the
349 positive impact of AM symbiosis on the host transcends nutrient acquisition [47]. Additionally,
350 phylogenomic studies of the symbiotic phosphate transporter PT4 suggest that this trait evolved
351 late and therefore that phosphorus acquisition might not have been the (only) driving force for the
352 emergence of AM symbiosis [44]. *SymRK* and *Ram1* were identified in the genomes of liverworts,
353 but evolution of *CCaMK* predated the emergence of all land plants, as shown by its presence and
354 conserved biochemical function in advanced charophytes [44]. Together, these findings raise
355 questions regarding the forces driving the evolution of signaling genes enabling intracellular
356 symbioses in land plants. Our study shows that in *L. japonicus*, simultaneous impairment of AM
357 and RN symbioses in *symrk* and *ccamk* plants had a dramatic effect on the composition of both
358 bacterial and fungal communities of the legume root microbiota (Fig. 5). Importantly, mutation of
359 *CCaMK* and *SymRK* led to an almost complete depletion of a large number of fungal OTUs, mostly
360 belonging to Glomeromycota, indicating that in *Lotus*, these genes predominantly control the
361 colonization of roots by this particular fungal lineage. The finding that *ram1-2* mutants show
362 retained accommodation for a subset of fungal root endophytes (n=13; Fig. 5B, and Fig 4B) whose
363 colonization is dependent on an intact common symbiosis pathway is not surprising based on the
364 capacity of these mutants to enable fungal colonization but not to sustain a full symbiotic
365 association [35], and indicates that *RAM1* is dispensable for the intraradical colonization of these

366 Glomeromycota fungi. Alternatively, these fungal root endophytes may engage in commensal
367 rather than mutualistic relationships with *L. japonicus* independently of the AM symbiosis pathway,
368 as is the case for multiple species of commensal non-symbiotic rhizobia [22,48]. Given that *ram1*
369 mutants specifically block AM arbuscule differentiation but not root colonization [35], it is
370 conceivable that the Glomeromycota taxa colonizing this plant genotype cannot form arbuscules
371 during root colonization.

372 Legumes have evolved the capacity to recognize and accommodate both types of intracellular
373 symbionts, and the large effect of CSSP genes on associated microbiota seen in the present work
374 could reflect a legume-specific trait. However, in rice, which does not engage in symbiotic
375 relationships with nodulating rhizobia, mutants lacking *CCaMK* were also found to display
376 significant changes in root-associated bacterial communities that could be mainly explained by
377 depletion of Rhizobiales and Sphingomonadales lineages [49]. Thus, our findings based on
378 comparative microbiota analysis of *Lotus ccamk* and *ram1* mutants suggest a broader role for
379 common symbiosis signaling genes in microbiota assembly. Future studies on orthologous genes
380 in basal land plants will contribute to a better understanding of the role of symbiotic signaling in the
381 evolution of plant-microbiota associations.

382 **Materials and Methods**

383 **Preparation and storage of soil**

384 The two soil batches used in this study were collected from Max Planck Institute for Plant Breeding
385 Research agricultural field located in Cologne, Germany (50.958N, 6.865E) in the following
386 seasons: CAS11-spring/autumn 2016, CAS12-spring 2017 (CAS: Cologne Agriculture Soil). The
387 field had not been cultivated in previous years, no fertilizer or pesticide administration took place at
388 the harvesting site. Following harvest, soil was sieved, homogenized and stored at 4 °C for further
389 use.

390 **Soil and plant material**

391 All studied *L. japonicus* symbiosis-deficient mutants, *nfr5-2* [33], *ram1-2* [35], *symrk-3* [7] and
392 *ccamk-13* [34], originated from the Gifu B-129 genotype.

393 **Plant growth and harvesting procedure**

394 The germination procedure of *L. japonicus* seeds included sandpaper scarification, surface
395 sterilisation in 1% hypochlorite bleach (20 min, 60 rpm), followed by three washes with sterile water
396 and incubation on wet filter paper in Petri dishes for one week (temperature: 20 °C, day/night cycle
397 16/8h, relative humidity: 60%). For each genotype and soil batch, six to eight biological replicas
398 were prepared by potting four plants in 7x7x9 cm pot filled with corresponding batch of soil (CAS11
399 soil six replicates, CAS12 soil eight replicated). For each batch of soil, two independent
400 experiments have been carried out. Plants were incubated for ten weeks in the greenhouse
401 (day/night cycle 16/8h, light intensity 6000 LUX, temperature: 20 °C, relative humidity: 60%), and
402 were watered with tap water twice per week.

403 The block of soil containing plant roots was removed from the pot and adhering soil was discarded
404 manually. Three sample pools were collected: complete root systems (harvested 1 cm below the
405 hypocotyl), upper fragments of the root systems (4 cm-long, starting 1 cm below the hypocotyl) and
406 lower root system fragments (harvested from 9 cm below; the latter two were collected from plants
407 grown in the same pot (Fig. 1a). All pools were washed twice with sterile water containing 0.02%
408 Triton X-1000 detergent and twice with pure sterile water by vigorous shaking for 1 min. The
409 rhizosphere compartment was derived by collection of pellet following centrifugation of the first
410 wash solution for 10 min at 1500 g. The nodules and visible primordia were separated from
411 washed root pools of nodulating genotypes (WT and ram1-2) with a scalpel and discarded. In order
412 to obtain the root compartment the root sample pools were sonicated to deplete the microbiota
413 fraction attached to the root surface. It included 10 cycles of 30-second ultrasound treatment
414 (Bioruptor NextGen UCD-300, Diagenode) for complete root systems and upper root fragments,
415 while for the lower root fragments the number of cycles was reduced to three. All samples were
416 stored at -80 °C for further processing. For AM colonisation inspection the whole root system of
417 washed soil-grown plants was stained with 5% ink in 5% acetic acid solution and inspected for
418 intraradical infection.

419 **Generation of 16S rRNA and ITS2 fragment amplicon libraries for Illumina MiSeq**
420 **sequencing**

421 Root pool samples were homogenized by grinding in a mortar filled with liquid nitrogen and
422 treatment with Precellys24 Tissue lyser (Bertin Technologies) for two cycles at 5600 rpm for 30
423 sec. DNA was extracted with the FastDNA Spin Kit for Soil, according to the manufacturer's
424 protocol (MP Bioproducts). DNA concentrations were measured fluorometrically (Quant-iT™
425 PicoGreen dsDNA assay kit, Life Technologies, Darmstadt, Germany), and adjusted to 3.5 ng/µl.

426 Barcoded primers targeting the variable V5-V7 region of the bacterial 16S rRNA gene (799F and
427 1193R, [29]) or targeting the ITS2 region of the eukaryotic ribosome (fITS7 and ITS4, [30,31]) were
428 used for amplification. The amplification products were purified, pooled and subjected to
429 sequencing with Illumina MiSeq equipment.

430 **Processing of 16S rRNA and ITS2 reads**

431 Libraries from the three root fractions (including root tips endosphere, upper root endosphere and
432 whole root endosphere) were analysed independently. As well as the main experiments (only
433 whole roots). Due to a very low read count for 16S data in the first experiment in CAS11 soil, this
434 data was not included in the final analysis. This resulted in an overall lower sample number for
435 bacteria than for fungi (222 vs. 274 samples). All sets of amplicon reads were processed as
436 recently described [32], using a combination of QIIME [50] and USEARCH tools [51]. For both
437 datasets paired end reads were used. For ITS2 data, forward reads were kept, in case that no
438 paired version was available. Main steps include quality filtering of reads, de-replicating, chimera
439 detection and OTU clustering at a 97% threshold. 16S reads were filtered against the greengenes
440 data base [52], whereas for ITS2 the reads where checked with ITSx [53] and compared against a
441 dedicated ITS database to remove ITS sequences from non-fungal species. Taxonomic
442 classification was done with uclust (assign_taxonomy from QIIME) for 16S OTUs and rdp classifier
443 [54] for ITS2 OTUs. For the sake of consistency with NCBI taxonomic classification, the
444 assignment of the ITS2 sequences was manually corrected so that that all OTUs assigned as
445 Ilyonectria were assigned as belonging to the Sordariomycetes, Hypocreales and Nectriaceae. For
446 16S data, OTUs assigned as mitochondrial or chloroplast, were removed prior to analysis.

447 **Statistical analysis**

448 For calculating Shannon diversity indices, OTU tables were rarefied to 1000 reads
449 (single_rarefaction.py from QIIME, samples with less than 1000 reads were omitted). Significant
450 differences were determined using ANOVA (aov function in R) and post-hoc Tukey test (TukeyHSD
451 in R, $p<0.05$). For calculating Bray Curtis distances between samples, OTU tables were
452 normalized using cumulative sum scaling (CSS, [55]). Bray-Curtis distances were used as input for
453 principal coordinate analysis (PCoA, cmdscale function in R) plots and as input for constrained
454 analysis of principal coordinate (CPCoA, capscale function, vegan package in R). For the latter, the
455 analysis was constrained by genotypes (each mutant and WT separately) and corrected for the
456 effect of the two soil types (CAS 11, CAS 12) and the four individual experiments (using the

457 “Condition” function). This analysis has been repeated with OTU tables from which OTUs that
458 represent known plant symbionts (Phyllobacteriaceae for 16S and Glomeromycota for ITS2) were
459 removed before normalization, distance calculation and CPCoA. A previously described approach
460 was used to draw ternary plots and for respective enrichment analysis [22]. Fold change of OTUs
461 between wild type and mutant plants was calculated as followed. Samples showing a read count
462 <5000 were removed. OTUs with mean relative abundance (RA) >0.1% across all root or
463 rhizosphere samples, respectively, were kept for analysis. Fold change in RA from WT to mutants
464 was calculated over all WT samples for *nfr5*, *ram1* and *symrk* whereas the change to *ccamk* was
465 only calculated with WT samples from experiments where *ccamk* mutants were present. To avoid
466 zeros in calculation the RA of OTUs missing from samples was set to 0.001%. The significance of
467 differences in abundance was tested using the Kruskal-Wallis test ($p<0.05$). Networks for each
468 genotype and kingdom were calculated independently using SparCC [37]. OTU tables were filtered
469 before analysis to only include samples from one soil type (CAS12) to avoid biases. In addition
470 only OTUs that are present in more than 10 samples and have mean RA >0.1% were kept for
471 network analysis. Raw count tables were given to SparCC as an input, the resulting correlations
472 were filtered by significance ($p < 0.05$). Networks were drawn using Cytoscape [56]. To calculate
473 the degree centrality, the number of positive and negative connections, for each OTU was divided
474 by the number of OTUs present in the respective network. Correlations between bacterial and
475 fungal OTUs were calculated as followed. OTUs that appear in less than 10 gifu root samples and
476 have mean RA < 0.1% were not considered for this analysis. Spearman rank correlations were
477 calculated between RA values of bacterial and fungal OTUs across all gifu root samples (cor.test
478 function in R, $p< 0.001$). For showing the cumulative correlation of bacterial OTUs to fungal OTUs,
479 the respective correlations for one bacterial OTU were summed up, so the number of correlations
480 and the strength could be accessed in one analysis. This was repeated, but just for fungal OTUs
481 annotated as Glomeromycota.

482

Acknowledgements

This work was supported by funds to S. R. from The Danish National Research Foundation (Grant no. DNRF79), by funds to P.S.-L. from the Max Planck Society, a European Research Council advanced grant (ROOTMICROBIOTA), the 'Cluster of Excellence on Plant Sciences' program funded by the Deutsche Forschungsgemeinschaft (DFG), and SPP 2125 DECRyPT from the DFG.

Conflict of interest

The authors declare no conflict of interests.

Data availability

All sequencing reads will be uploaded to the European Nucleotide Archive (ENA). Code and relevant data files (e.g. OTU tables) will be made public via GitHub.

495 **References**

496 1. Remy W, Taylor TN, Hass H, Kerp H. Four hundred-million year-old vesicular arbuscular
497 mycorrhizae. *Proc Natl Acad Sci USA* 91 1994; 11:841–11.

498 2. Taylor TN, Remy W, Hass H, Kerp H. Fossil Arbuscular Mycorrhizae from the Early Devonian.
499 *Mycologia* 1995; 87(4):560-573.

500 3. Pirozynski KA, Malloch DW. The origin of land plants: a matter of mycotrophism. *Biosystems*
501 1975; 6:153-164.

502 4. Smith SE, Read D J,Vesicular-arbuscular mycorrhizas in agriculture and horticulture. In
503 *Mycorrhizal Symbiosis* . Academic press,1997. (pp. 453-469).

504 5. Wang B, Qiu YL. Phylogenetic distribution and evolution of mycorrhizas in land plants.
505 *Mycorrhiza* 2006; 16(5):299-363.

506 6. Bonfante P, Genre A. Mechanisms underlying beneficial plant-fungus interactions in mycorrhizal
507 symbiosis. *Nat Commun* 2010; 1:48.

508 7. Stracke S, Kistner C, Yoshida S, Mulder L, Sato S, Kaneko T, et al. A plant receptor-like kinase
509 required for both bacterial and fungal symbiosis. *Nature* 2002; 417(6892):959-62

510 8. Antolin-Llovera M, Ried MK, Parniske M. Cleavage of the SYMBIOSIS RECEPTOR-LIKE
511 KINASE ectodomain promotes complex formation with Nod factor receptor 5. *Curr Biol* 2014;
512 24(4):422-427.

513 9. Charpentier M, Bredemeier R, Wanner G, Takeda N, Schleiff E, Parniske M. Lotus japonicus
514 CASTOR and POLLUX are ion channels essential for perinuclear calcium spiking in legume root
515 endosymbiosis. *Plant Cell* 2008; 20(12).

516 10. Ane JM, Kiss GB, Riely BK, Penmetsa RV, Oldroyd GE, Ayax C. Medicago truncatula DMI1
517 required for bacterial and fungal symbioses in legumes. *Science* 2004; 303(5662):1364-1367.

518 11. Kanamori N, Madsen LH, Radutoiu S, Frantescu M, Quistgaard EM, Miwa H. A nucleoporin is
519 required for induction of Ca2+ spiking in legume nodule development and essential for rhizobial
520 and fungal symbiosis. *Proc Natl Acad Sci* USA 2006; 103(2):59-364

521 12. Saito K, Yoshikawa M, Yano K, Miwa H, Uchida H, Asamizu E. NUCLEOPORIN85 is
522 required for calcium spiking, fungal and bacterial symbioses, and seed production in Lotus
523 japonicus. *Plant Cell* 2007; 19(2):610-624

524 13. Groth M, Takeda N, Perry J, Uchida H, Draxl S, Brachmann A. NENA, a Lotus japonicus
525 homolog of Sec13, is required for rhizodermal infection by arbuscular mycorrhiza fungi and
526 rhizobia but dispensable for cortical endosymbiotic development. *Plant Cell* 2010; 22(7):2509-
527 2526.

528

529 14. Charpentier M, Sun J, Vaz Martins T, Radhakrishnan GV, Findlay K, Soumpourou E. Nuclear-
530 localized cyclic nucleotide-gated channels mediate symbiotic calcium oscillations. Science 2016;
531 352(6289):1102-1105.

532 15. Levy J, Bres C, Geurts R, Chalhoub B, Kulikova O, Duc G. A putative Ca2+ and calmodulin-
533 dependent protein kinase required for bacterial and fungal symbioses. Science 2004;
534 303(5662):1361-1364.

535 16. Mitra RM, Gleason CA, Edwards A, Hadfield J, Downie JA, Oldroyd GE, et al. A
536 Ca2+/calmodulin-dependent protein kinase required for symbiotic nodule development: Gene
537 identification by transcript-based cloning. *Proc Natl Acad Sci U S A* 2004; 101(13):4701-5.

538 17. Yano K, Yoshida S, Muller J, Singh S, Banba M, Vickers K. et al. CYCLOPS, a mediator of
539 symbiotic intracellular accommodation. *Proc Natl Acad Sci U S A* 2008; 105(51):20540-20545.

540 18. Singh S, Katzer K, Lambert J, Cerri M, Parniske M. CYCLOPS, a DNA-binding transcriptional
541 activator, orchestrates symbiotic root nodule development. *Cell Host Microbe* 2014; 15(2):139-152.

542 19. Messinese E, Mun JH, Yeun LH, Jayaraman, D, Rouge P, Barre, A, et al. A novel nuclear
543 protein interacts with the symbiotic DMI3 calcium- and calmodulin-dependent protein kinase of
544 Medicago truncatula.. *Mol Plant Microbe Interact* 2007; 20(8):912-921.

545 20. Udvardi M, Poole PS. Transport and metabolism in legume-rhizobia symbioses. *Annu Rev Plant*
546 *Biol* 2013; 64:781-805.

547 21. Gutjahr C, Sawers RJH, Marti G, Andres-Hernandez L, Yang S, Casieri L. Transcriptome
548 diversity among rice root types during asymbiosis and interaction with arbuscular mycorrhizal
549 fungi. *Proc Natl Acad Sci* USA 2015; 112(21):6754.

550 22. Zgadzaj R, Garrido-Oter R, Jensen DB, Koprivova A, Schulze-Lefert P, Radutoiu S. Root
551 nodule symbiosis in Lotus japonicus drives the establishment of distinctive rhizosphere, root, and
552 nodule bacterial communities. *Proc Natl Acad Sci U S A* 2016; 113(49):E7996-E8005.

553 23. Johnson D, Gilbert L. Interplant signalling through hyphal networks. New Phytol 2014;
554 205(4):1448-53.

555 24. Hassani MA, Duran, P, Hacquard S. Microbial interactions within the plant holobiont.
556 *Microbiome* 2018; 6(1):58.

557 25. Xue L, Almario J, Fabianska I, Saridis G, Bucher M. Dysfunction in the arbuscular mycorrhizal
558 symbiosis has consistent but small effects on the establishment of the fungal microbiota in *Lotus*
559 *japonicas*. New Phytol 2019;

560 26. Chabaud M, Genre A, Sieberer BJ, Faccio A, Fournier J, Novero M, et al. Arbuscular
561 mycorrhizal hyphopodia and germinated spore exudates trigger Ca2+ spiking in the legume and
562 nonlegume root epidermis. *New Phytol* 2011; 189(1):347-5.

563 27. Miwa H, Sun J, Oldroyd GE, Downie JA. Analysis of calcium spiking using a cameleon
564 calcium sensor reveals that nodulation gene expression is regulated by calcium spike number and
565 the developmental status of the cell. *Plant J* 2006; 48(6):883-94.

566 28. Bulgarelli D, Rott M, Schlaeppi K, Emiel Ver Loren van Themaat E, Ahmadinejad N, Assenza
567 F, et al. Revealing structure and assembly cues for Arabidopsis root-inhabiting bacterial microbiota.
568 *Nature* 2012; 488:91-95.

569 29. Schlaeppi K, Dombrowski N, Oter RG, Ver Loren van Themaat E, Schulze-Lefert P.
570 Quantitative divergence of the bacterial root microbiota in Arabidopsis thaliana relatives. *Proc Natl*
571 *Acad Sci U S A* 2014; 111(2):585-92.

572 30. Ihrmark K, Bödeker IT, Cruz-Martinez K, Friberg H, Kubartova A, Schenck J,et al. New
573 primers to amplify the fungal ITS2 region--evaluation by 454-sequencing of artificial and natural
574 communities. *FEMS Microbiol Ecol* 2012; 82(3):666-77.

575 31. White TJ, Bruns TD, Lee SB, Taylor JW. Amplification and direct sequencing of fungal
576 ribosomal RNA genes for phylogenetics. In: Innis MA, Gelfand DH, Sninsky JJ, White TJ, editors.
577 *PCR protocols: a guide to methods and applications*. United States: Academic Press, CA, USA,
578 1990, pp. 315-322.

579 32. Duran, P., Thiergart T, Garrido-Oter R, Agler M, Kemen E, Schulze-Lefert P, et al. (2018).
580 Microbial interkingdom interactions in roots promote Arabidopsis survival. *Cell* 2018; 175(4):973-
581 983.

582 33. Madsen EB, Madsen, LH, Radutoiu S, Olbryt M, Rakwalska M, Szczyglowski K, et al. A
583 receptor kinase gene of the LysM type is involved in legume perception of rhizobial signals. *Nature*
584 2003; 425(6958):637.

585 34. Perry J, Brachmann A, Welham T, Binder A, Charpentier M, Groth M, et al. TILLING in Lotus
586 japonicus identified large allelic series for symbiosis genes and revealed a bias in functionally
587 defective ethyl methanesulfonate alleles toward glycine replacements. *Plant Physiol* 2009; 151:
588 1281–1291.

589 35. Xue L, Cui H, Buer B, Vijayakumar V, Delaux PM, Junkermann S, et al. Network of GRAS
590 transcription factors involved in the control of arbuscule development in Lotus japonicus. *Plant*
591 *Physiol* 2015; 167(3):854-871.

592 36. Anderson MJ, Willis TJ, Canonical analysis of principal coordinates: A useful method of
593 constrained ordination for ecology. *Ecology* 2003; 84(2):511-525.

594 37. Friedman J, Alm EJ. Inferring correlation networks from genomic survey data. *PLoS*
595 *computational biology* 2012;8(9)

596 38. Lombard L, van der Merwe NA, Groenewald JZ, Crous PW. Generic concepts in Nectriaceae.
597 *Stud Myco*l 2015; 80:189-245.

598 39. Lofgren LA, LeBlanc NR, Certano AK, Nachtigall J, LaBine KM, Riddle J, et al. Fusarium
599 graminearum: pathogen or endophyte of North American grasses? *New Phytol* 2018; 217(3):1203-
600 1212.

601 40. Amselem J, Cuomo CA, van Kan, JA, Viaud M, Benito EP, Couloux A, et al. Genomic analysis
602 of the necrotrophic fungal pathogens Sclerotinia sclerotiorum and Botrytis cinerea. *PLoS Genet*
603 2011; 7(8).

604 41. Almario J, Jeena G, Wunder J, Langen G, Zuccaro A, Coupland G, Bucher M. Root-associated
605 fungal microbiota of nonmycorrhizal Arabis alpina and its contribution to plant phosphorus
606 nutrition. *Proc Natl Acad Sci U S A* 2017; 114(44):E9403-E9412.

607 42. Desiro A, Salvioli A, Ngonkeu EL, Mondo SJ, Epis S, Faccio A, et al. Detection of a novel
608 intracellular microbiome hosted in arbuscular mycorrhizal fungi. *ISME J* 2014; 8(2): 257-270.

609 43. Bianciotto V, Lumini E, Lanfranco L, Minerdi D, Bonfante P, Perotto S. Detection and
610 identification of bacterial endosymbionts in arbuscular mycorrhizal fungi belonging to the family
611 Gigasporaceae. *Appl Environ Microbiol* 2000;66(10):4503-4509.

612 44. Delaux PM, Radhakrishnan GV, Jayaraman D, Cheema J, Malbreil M, Volkening JD,et al.
613 Algal ancestor of land plants was preadapted for symbiosis. *Proc Natl Acad Sci U S A* 2015;
614 112(43):13390-13395.

615 45. Javot H, Penmetsa RV, Terzaghi N, Cook DR, Harrison MJ. A Medicago truncatula phosphate
616 transporter indispensable for the arbuscular mycorrhizal symbiosis. *Proc Natl Acad Sci U S A* 2007;
617 104(5):1720-5.
618
619 46 Sawers RJ, Svane SF, Quan C, Grønlund M, Wozniak B, Gebreselassie MN, et al. Phosphorus
620 acquisition efficiency in arbuscular mycorrhizal maize is correlated with the abundance of root-
621 external hyphae and the accumulation of transcripts encoding PHT1 phosphate transporters. *New*
622 *Phytol* 2017; 214(2):632-643.
623
624 47. Chen M, Arato M, Borghi L, Nouri E, Reinhardt D. Beneficial Services of Arbuscular
625 Mycorrhizal Fungi - From Ecology to Application. *Front Plant Sci* 2018; 9:1270.

626 48. Garrido-Oter R, Nakano RT, Dombrowski N, Ma KW, AgBiome T, McHardy AC, et al.
627 Modular Traits of the Rhizobiales Root Microbiota and Their Evolutionary Relationship with
628 Symbiotic Rhizobia. *Cell Host Microbe* 2018; 24(1):155-167 e155.

629 49. Ikeda S, Okubo T, Takeda N, Banba M, Sasaki K, Imaizumi-Anraku H, et al. The genotype of
630 the calcium/calmodulin-dependent protein kinase gene (CCaMK) determines bacterial community
631 diversity in rice roots under paddy and upland field conditions. *Appl Environ Microbiol* 2011;
632 77(13):4399-4405.

633 50. Caporaso JG, Kuczynski J, Stombaugh J, Bittinger K, Bushman FD, Costello EK, et al. QIIME
634 allows analysis of high-throughput community sequencing data. *Nat Methods* 2010; 7:335-336.

635 51. Edgar RC. UPARSE: highly accurate OTU sequences from microbial amplicon reads. *Nat*
636 *Methods* 2013; 10:996-998.

637 52. DeSantis TZ, Hugenholtz P, Larsen N, Rojas M, Brodie EL, Keller K, et al. Greengenes, a
638 chimera-checked 16S rRNA gene database and workbench compatible with ARB. *Appl Environ*
639 *Microbiol* 2006; 72:5069-5072

640 53. Bengtsson-Palme J, Ryberg M, Hartmann M, Branco S, Wang Z, Godhe A, De Wit P, et al.
641 Improved software detection and extraction of ITS1 and ITS2 from ribosomal ITS sequences of
642 fungi and other eukaryotes for analysis of environmental sequencing data. *Methods Ecol Evol* 2013;
643 4: 914-919.

644 54. Wang Q, Garrity GM, Tiedje JM, Cole JR. Naive Bayesian classifier for rapid assignment of
645 rRNA sequences into the new bacterial taxonomy. *Appl Environ Microb* 2007; 73:5261-5267.

646 55. Paulson, JN, Stine, OC, Bravo HC, Pop M. Differential abundance analysis for microbial
647 marker-gene surveys. *Nat Methods* 2013; 10:1200-1202.

648 56. Shannon P, Markiel A, Ozier O, Baliga NS, Wang JT, Ramage D, et al. Cytoscape: a software
649 environment for integrated models of biomolecular interaction networks. *Genome Research* 2003;
650 13(11),2498-2504.

651

652

653

654

655

656

657

658

659

660

661

662

663

Fig. 1

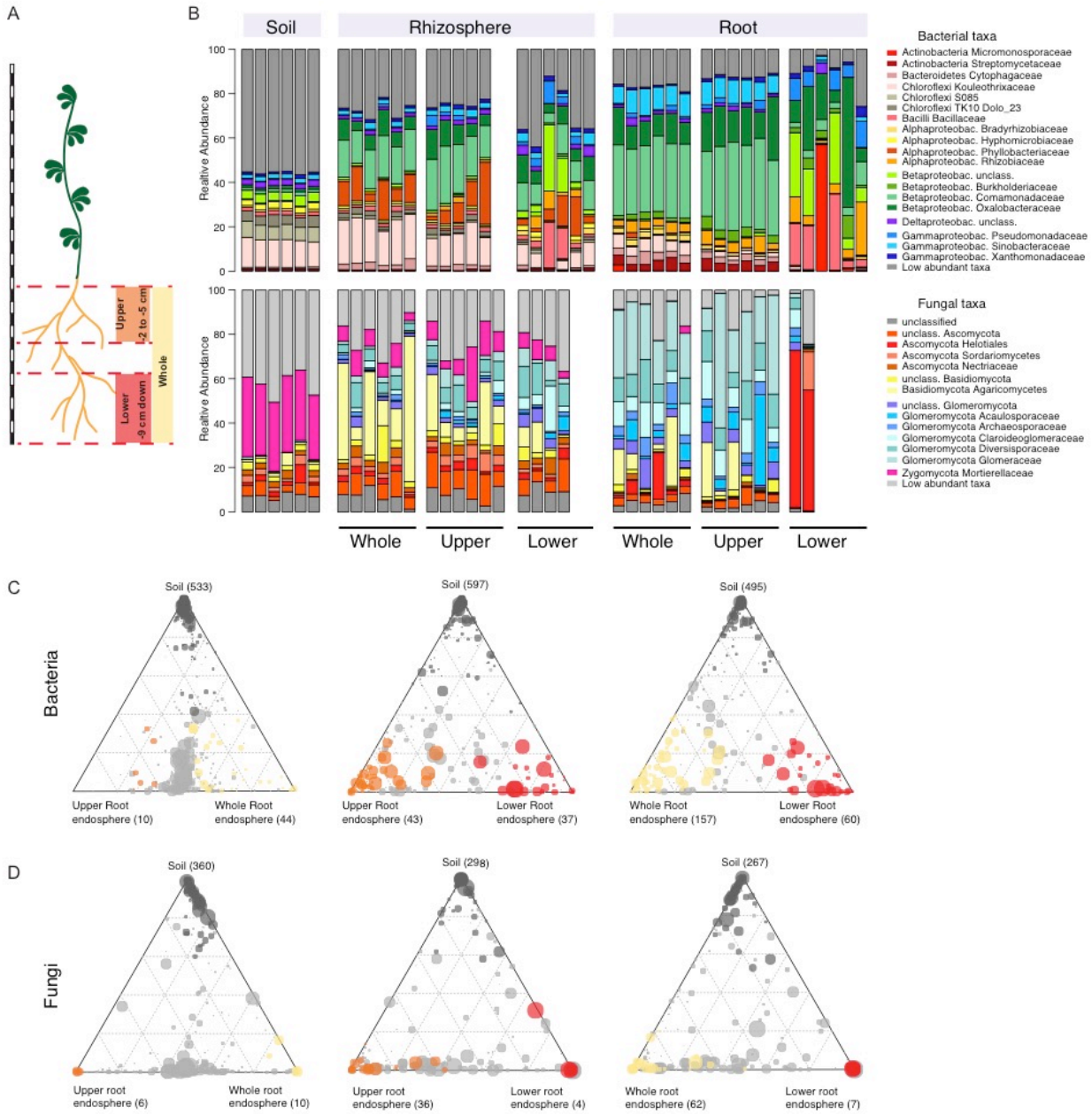

Fig1, **Bacterial & fungal community profile for different root fractions of *L. japonicus***.
A) Cartoon showing the length of the three different root fractions. B) Community profile showing the relative abundance of bacterial (upper panel) and fungal (lower panel) families across compartments and fractions (only samples with >5000 (bacteria) or >1000 (fungi) reads are shown, taxa having average RA < 0.1 (bacteria) or <0.15 (fungi) across all samples are aggregated as low-abundant.). C) Ternary plots showing bacterial OTUs that are enriched in the endosphere of specific root fractions, compared to the soil samples. B) Ternary plots showing fungal OTUs that are enriched in the endosphere of specific root fractions, compared to the soil samples. Circle size corresponds to RA across all fractions. Dark grey circles denote OTUs that are enriched in soil, light grey circles always represent OTUs that are not enriched in any of the fractions.

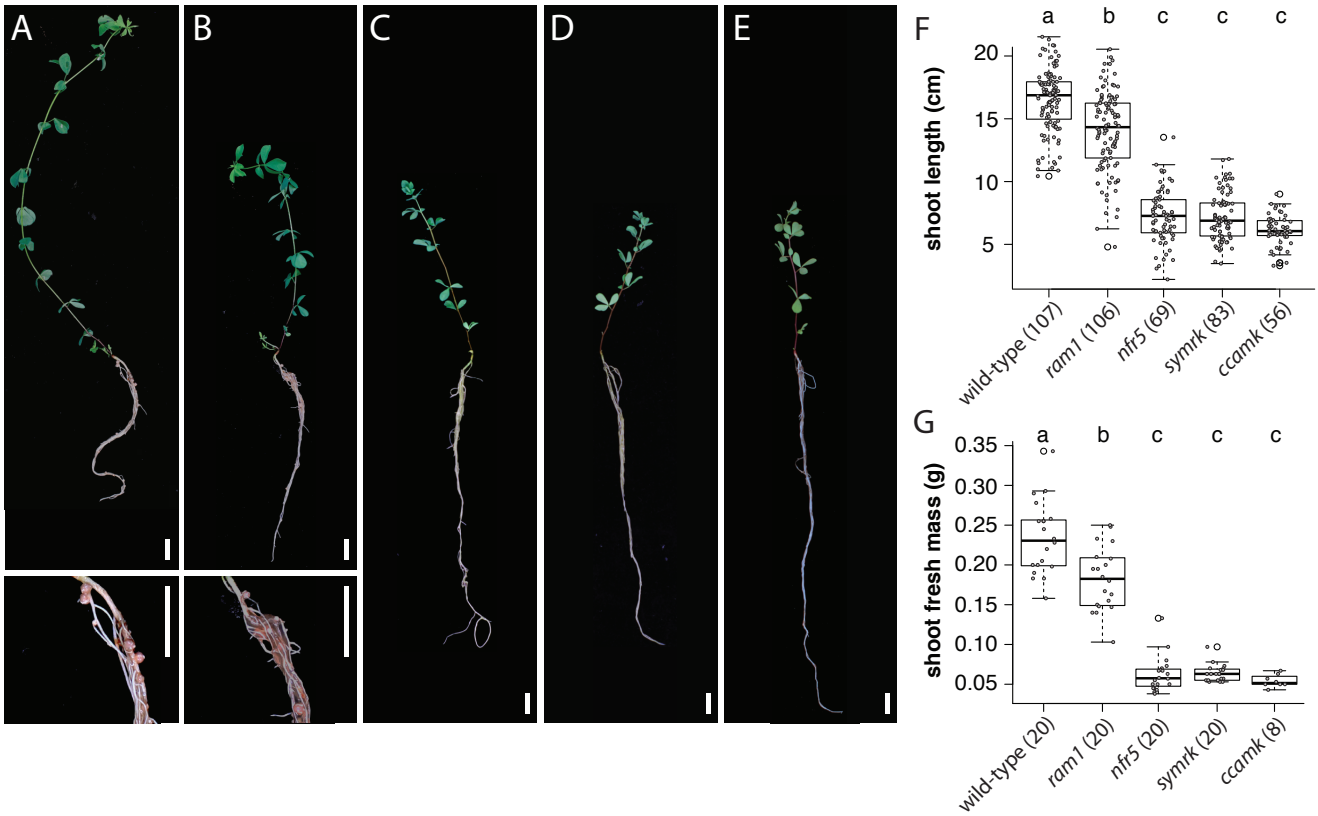

Fig2, **Phenotypes of WT and mutant plants**. Images depicting *L. japonicus* wild-type (A) and symbiosis-deficient mutant plants: *ram1* (B), *nfr5* (C), *symrk* (D) and *ccamk* (E). Insets show close-up view of nodules. Scale bars correspond to 1 cm. F) Boxplots display the shoot length for the identical set of genotypes presented in (A-E). G) Boxplots displaying the shoot fresh mass. Letters above plots correspond to groups based on Tukey's HSD test (P<0.05). Number of samples are indicated in brackets.

Fig. 3

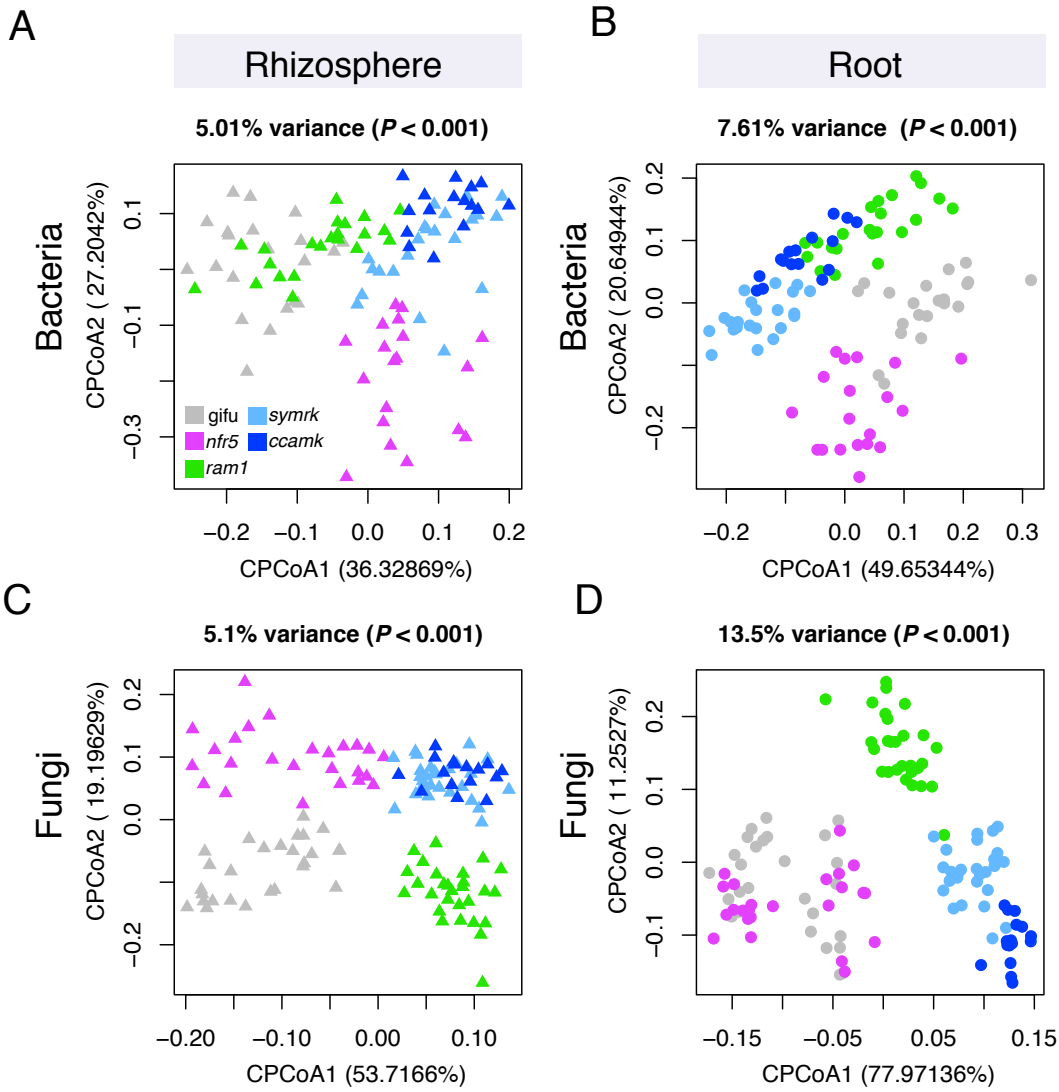

Fig3, **Constrained PCoA analysis showing genotype effect on microbial communities.** A) Constrained PCoA plots for bacterial datasets showing rhizosphere samples (n = 100) and B) root samples (n = 100). C) Constrained PCoA plots for fungal datasets showing only rhizosphere samples (n = 124) and D) root samples (n = 122).

Fig. 4

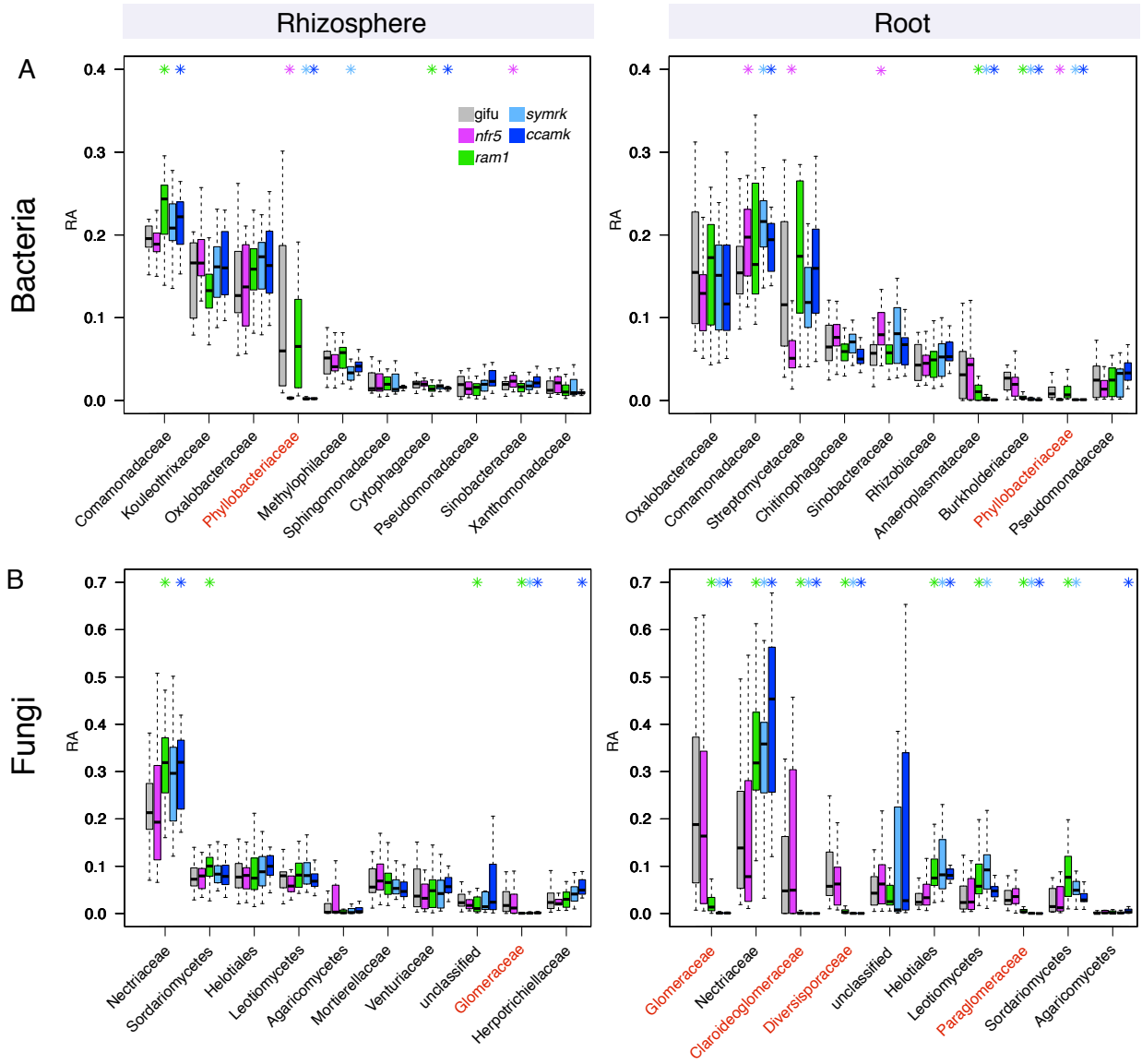

Fig4, **Relative abundance for main microbial taxa across plant compartments and genotypes**. A) RA for bacterial families in rhizosphere (left panel) and root compartment (right panel). B) RA for fungal families in rhizosphere (left panel) and root compartment (right panel). Taxa are sorted in decreasing order according to their average RA in wt plants (only first 10 most abundant taxonomical groups are shown). RA in wt as well as in the respective mutants is displayed. Significant differences compared to wt are marked with an asterisk in the color of the mutant ($P<0.05$, Kruskal-Wallis test). Families that include known symbionts are marked in red (Phyllobacteriaceae for bacteria and Glomeromyctes for Fungi). For some fungal taxa the next higher rank is shown, when no family level information was available.

Fig. 5

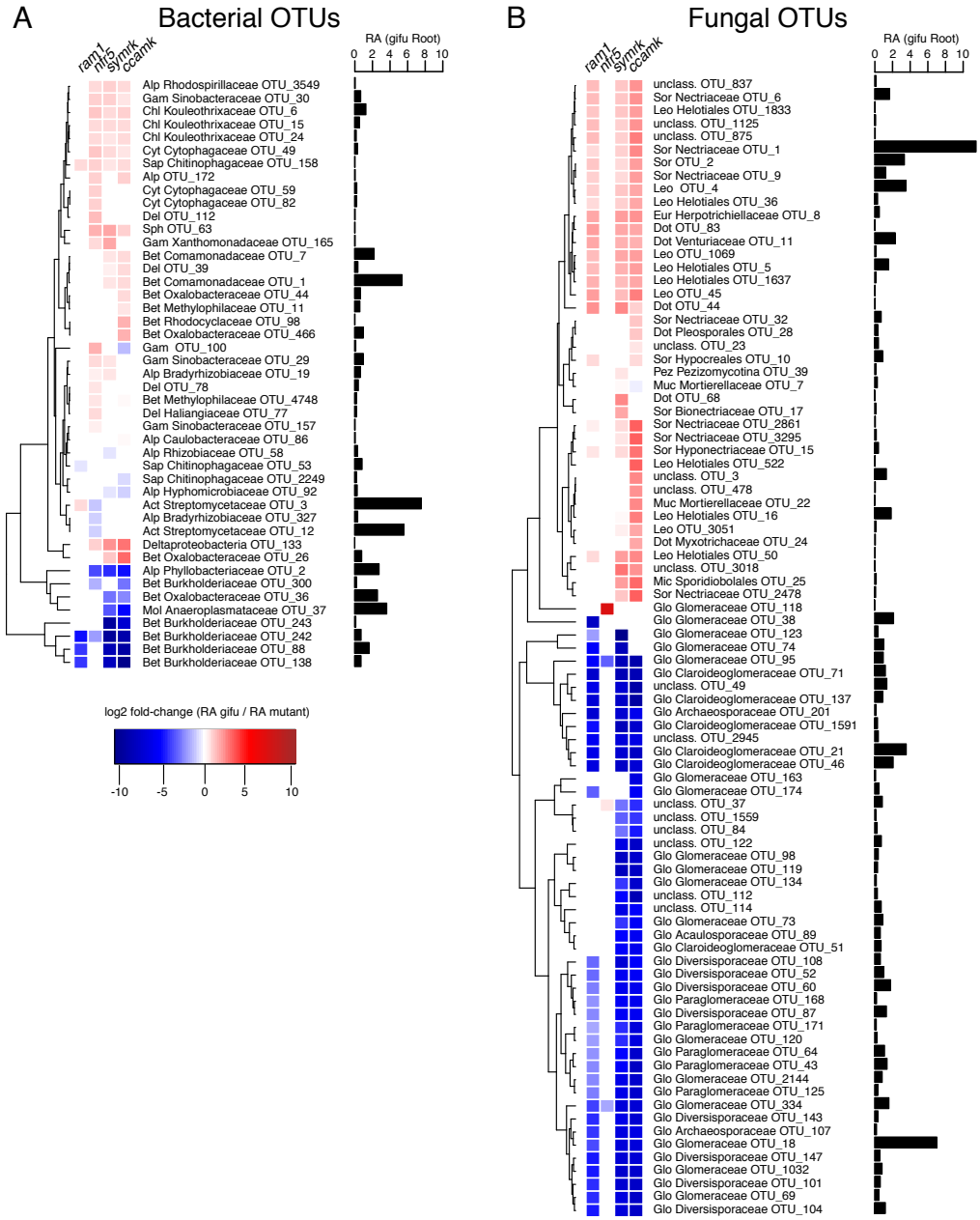

Fig5, **Differential abundance analysis for root associated OTUs**.
A) Bacterial OTUs that are differentially abundant in the roots of mutants compared to wt roots. B) fungal OTUs that are differentially abundant in the roots of mutants compared to wt roots. Only OTUs that have an average RA > 0.1% across all root samples, including mutants, are considered here. For each OTU the fold change in RA from wt to mutant is indicated (P <0.05, Kruskal-Wallis test). Next to each OTU the RA in wt roots is indicated. Phylum and family asscociation (if available) is given for each OTU (Bacterial phyla: Del=Deltaproteobactria, Gem=Gemm-1 , Chl=Chloroflexi, Bet=Betaproteobacteria, Alp=Alphaproteobacteria, Gam=Gammaproteobacteria, Cyt=Cytophagia, Sap=Saprospirae, Ped=Pedosphaerae, Sph= Sphingobacteria, Mol= Mollicutes ; Fungal phyla: Sor=Sordariomyctes, Dot=Dothideomycetes, Mic= Microbotryomycetes, Ust=Ustilaginomycetes, Eur=eurotiomycetes, Leo=Leotiomycetes, Aga=Agaricomycetes, Glo=Glomeromyctes, Pez=Pezizomycota, Muc=Mucoromycotina).

743 **Supplementary Figures**
744

Fig. S1

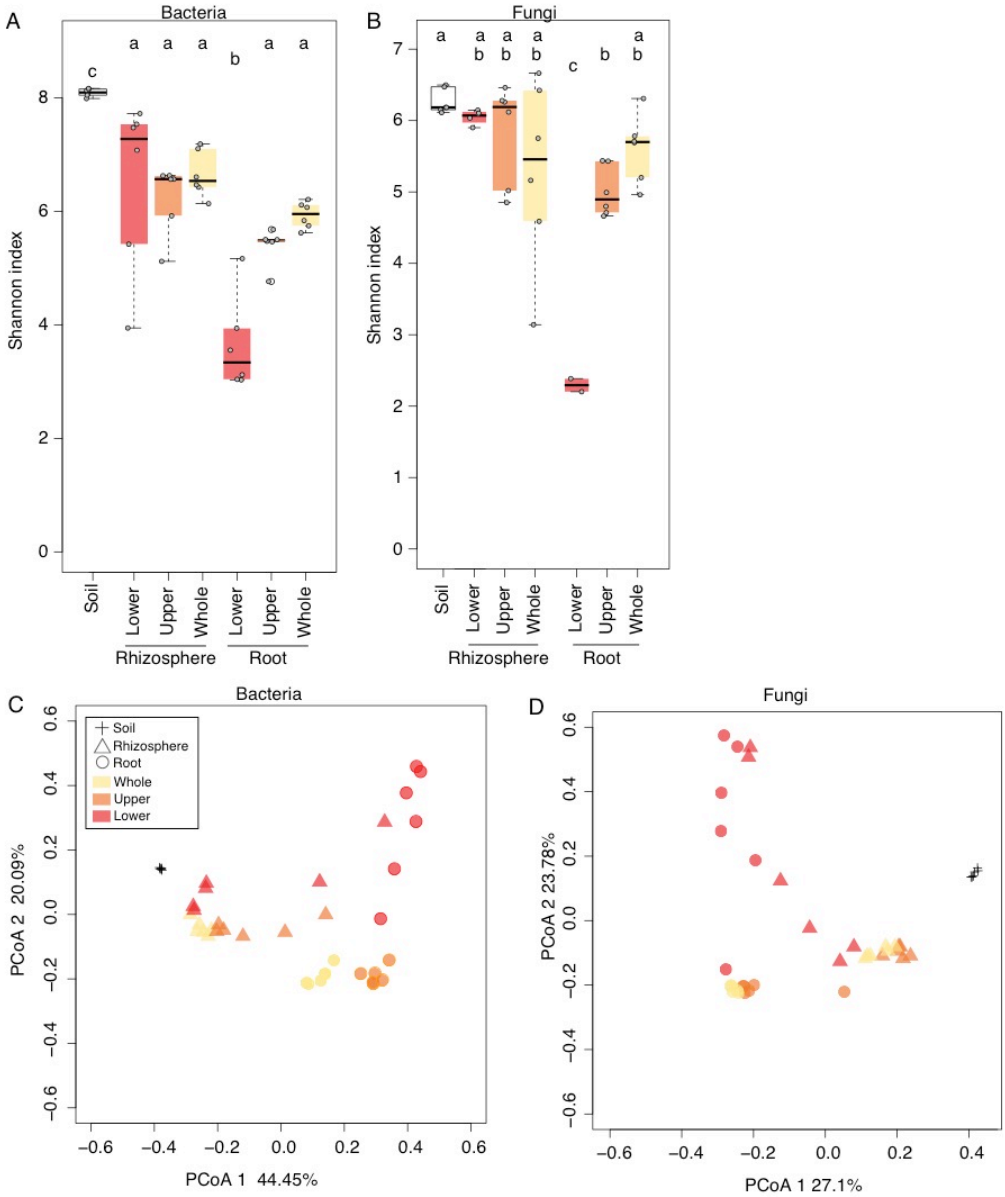

745
746
747
748
749 **Supp Fig1, Alpha and beta diversity across root fractions.**
750 A) Shannon diversity index for 16S amplicon data, soil (n=6), lower (n=6), upper (n=6), whole root
751 fractions (n=6), and respective rhizosphere samples (n=6 each) B) Shannon diversity index for
752 ITS2 amplicon data, soil (n=6), lower (n=2), upper (n=6), whole root fractions (n=6), and
753 respective rhizosphere samples (n=6 each, except lower, n=4) (ANOVA with Tukey's post hoc
754 test, P<0.05). C) Principal coordinate analysis of Bray-Curtis distances for bacterial data. D)
755 Principal coordinate analysis of Bray-Curtis distances for fungal data.
756
757

Fig. S2

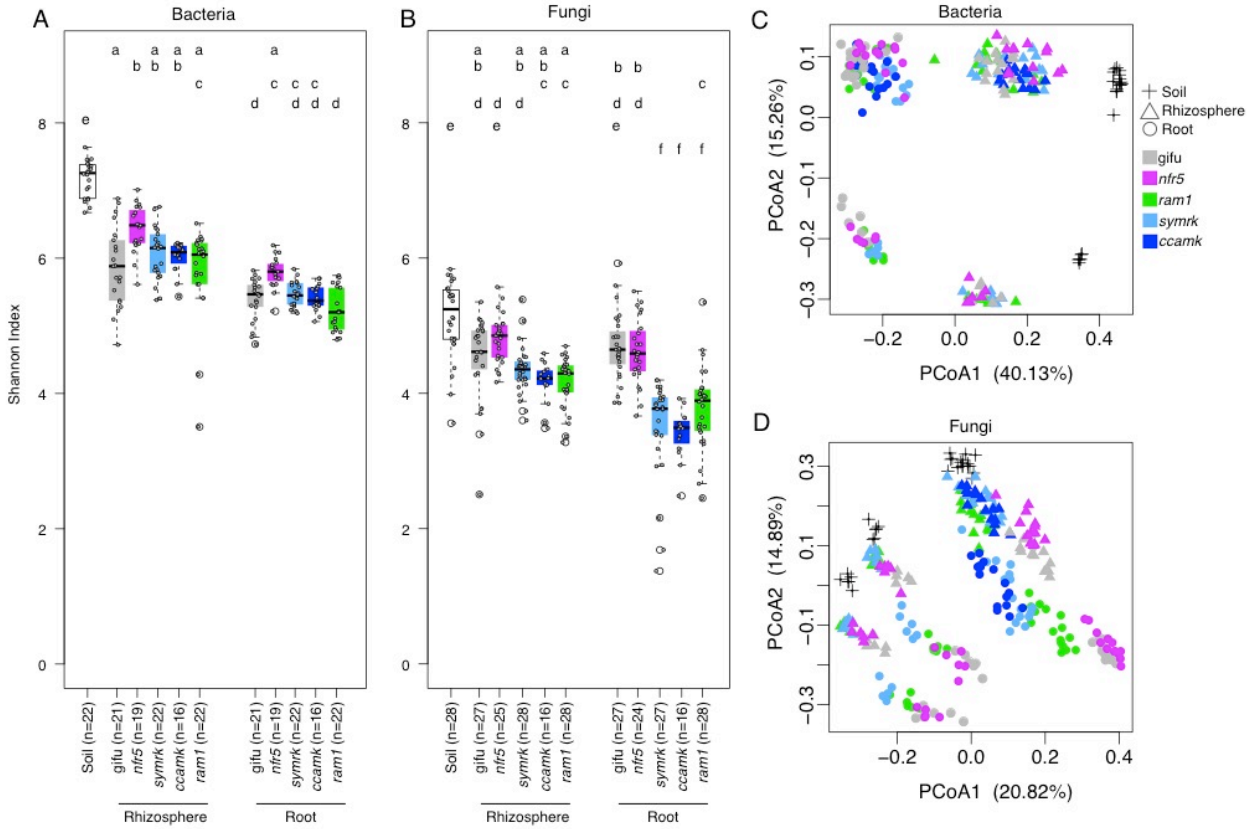

Supp Fig2, Alpha and beta diversity across plant compartments and genotypes.
A) Shannon diversity indices for the bacterial (16S amplicon) dataset. B) Shannon diversity indices for the fungal (ITS2 amplicon) dataset (ANOVA with Tukey's post hoc test, P<0.05) C) Principal coordinate analysis of Bray-Curtis distances for the bacterial dataset (n=222). D) Principal coordinate analysis of Bray-Curtis distances for the fungal dataset (n=274).

Fig. S3

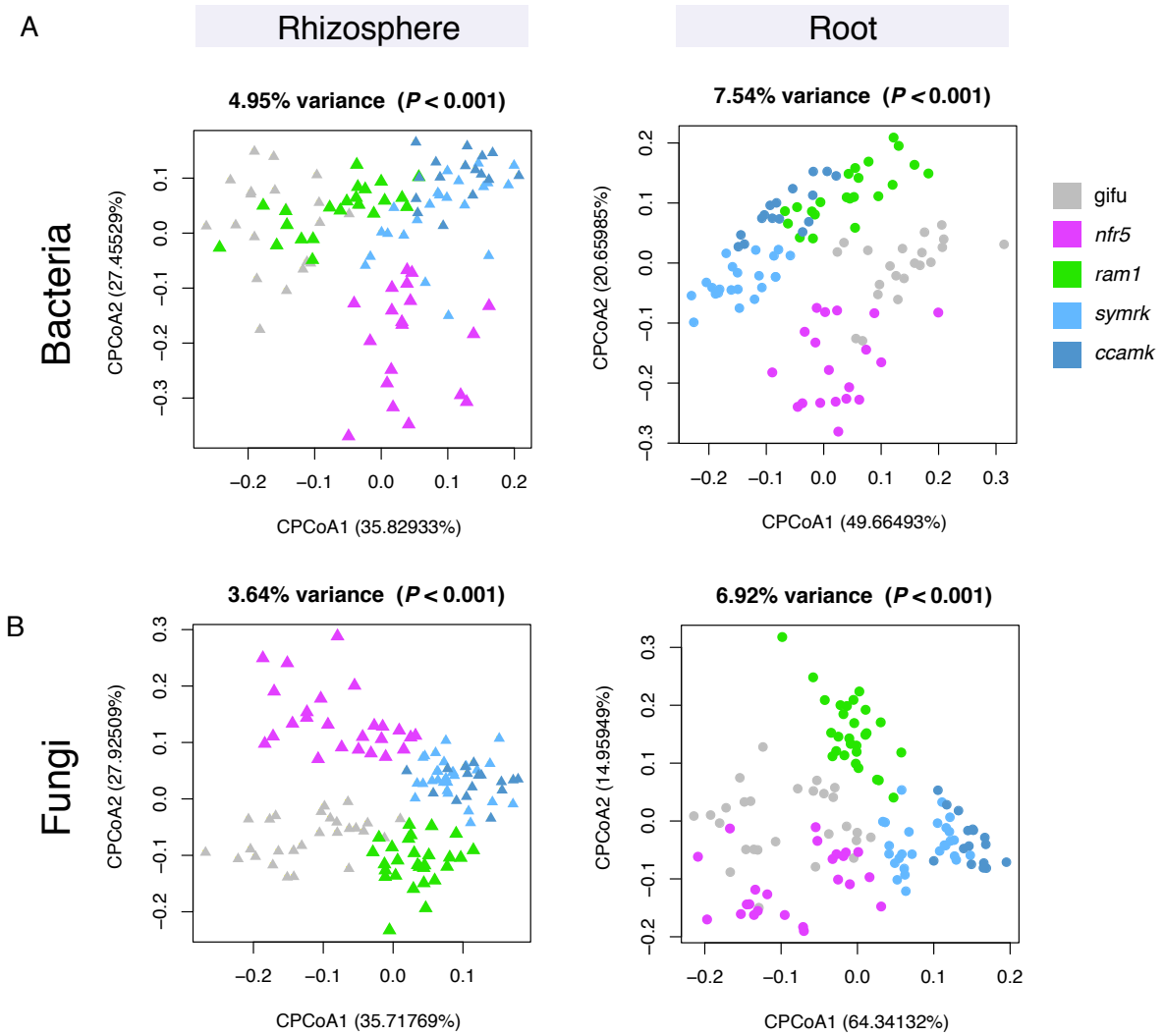

Supp Fig3, CPCoA with in-silico depletion of known symbionts. Results are separated by compartments. Datasets were constrained by genotype, and filtered for effects of experiments and soil type. A) Bacterial dataset from which OTUs belonging to the Phyllobacteriaceae were removed before analysis (root n=100, rhizosphere n=100). B) Fungal dataset from which OTUs belonging to the Glomeromycota were removed before analysis (root n=122, rhizosphere n=124).

Fig. S4

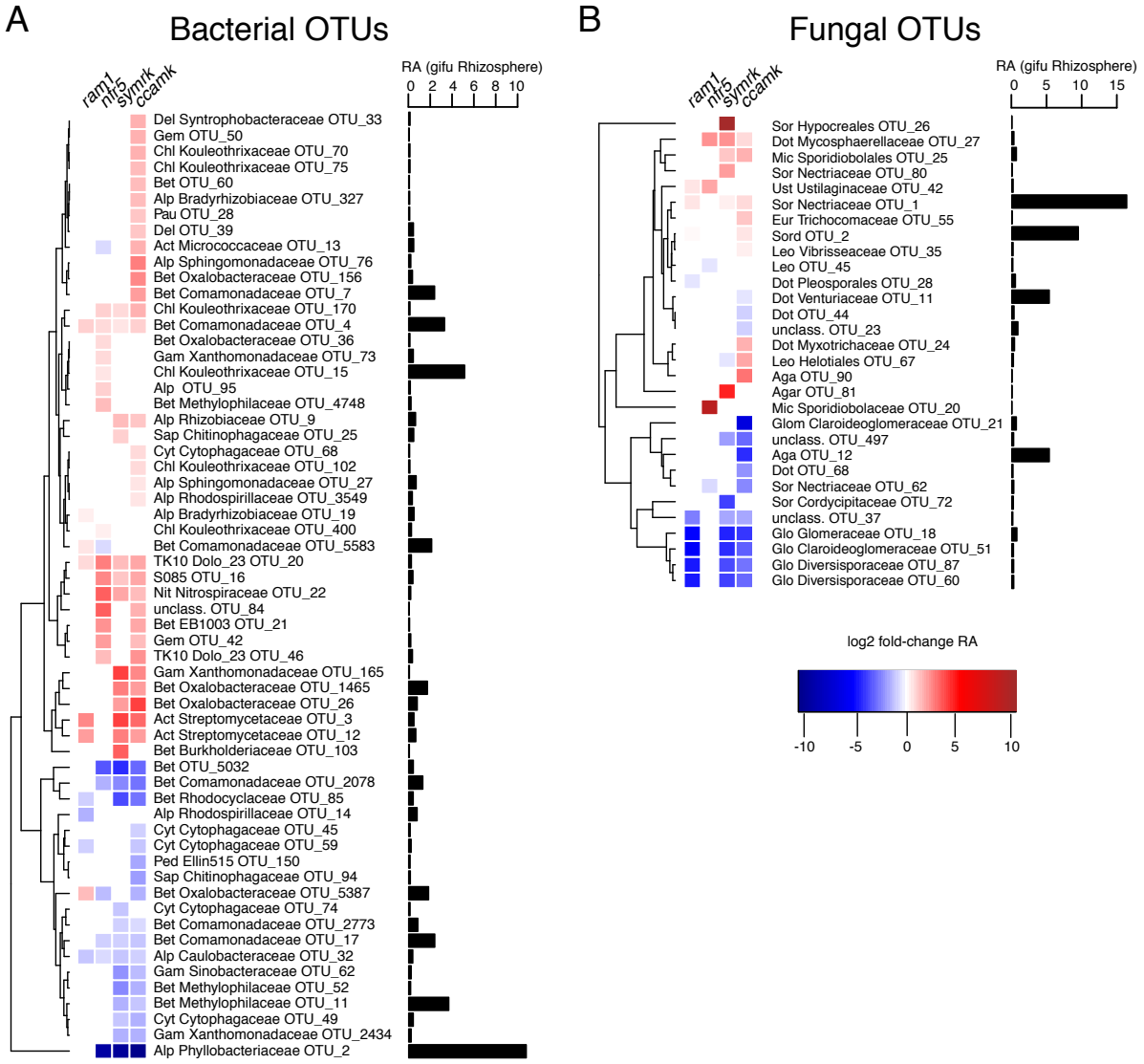

Supp Fig4, Differential abundance analysis for rhizosphere-associated OTUs showing enrichment and depletion in mutants.A) Bacterial OTUs that are differentially abundant in the rhizosphere of mutants compared to wt. B) Fungal OTUs that are differentially abundant in the rhizosphere of mutants compared to wt. Only OTUs that have an average RA > 0.1% across all rhizosphere samples, including mutants, are considered here. For each OTU, the fold change in RA from wt to mutant is indicated (P <0.05, Kruskal-Wallis test). Next to each OTU the RA in wt rhizosphere is indicated. Phylum and family asscociation is given for each OTU (Bacterial phyla: Del=Deltaproteobacteria, Gem=Gemm-1 , Chl=Chloroflexi, Bet=Betaproteobacteria, Alp=Alphaproteobacteria, Gam=Gammaproteobacteria, Cyt=Cytophagia, Sap=Saprospirae, Ped=Pedosphaerae, Sph= Sphingobacteria, Mol= Mollicutes ; Fungal phyla: Sor=Sordariomyctes, Dot=Dothideomycetes, Mic= Microbotryomycetes, Ust=Ustilaginomycetes, Eur=Eurotiomycetes, Leo=Leotiomycetes, Aga=Agaricomycetes, Glo=Glomeromyctes, Pez=Pezizomycota, Muc=Mucoromycotina).

Fig. S5

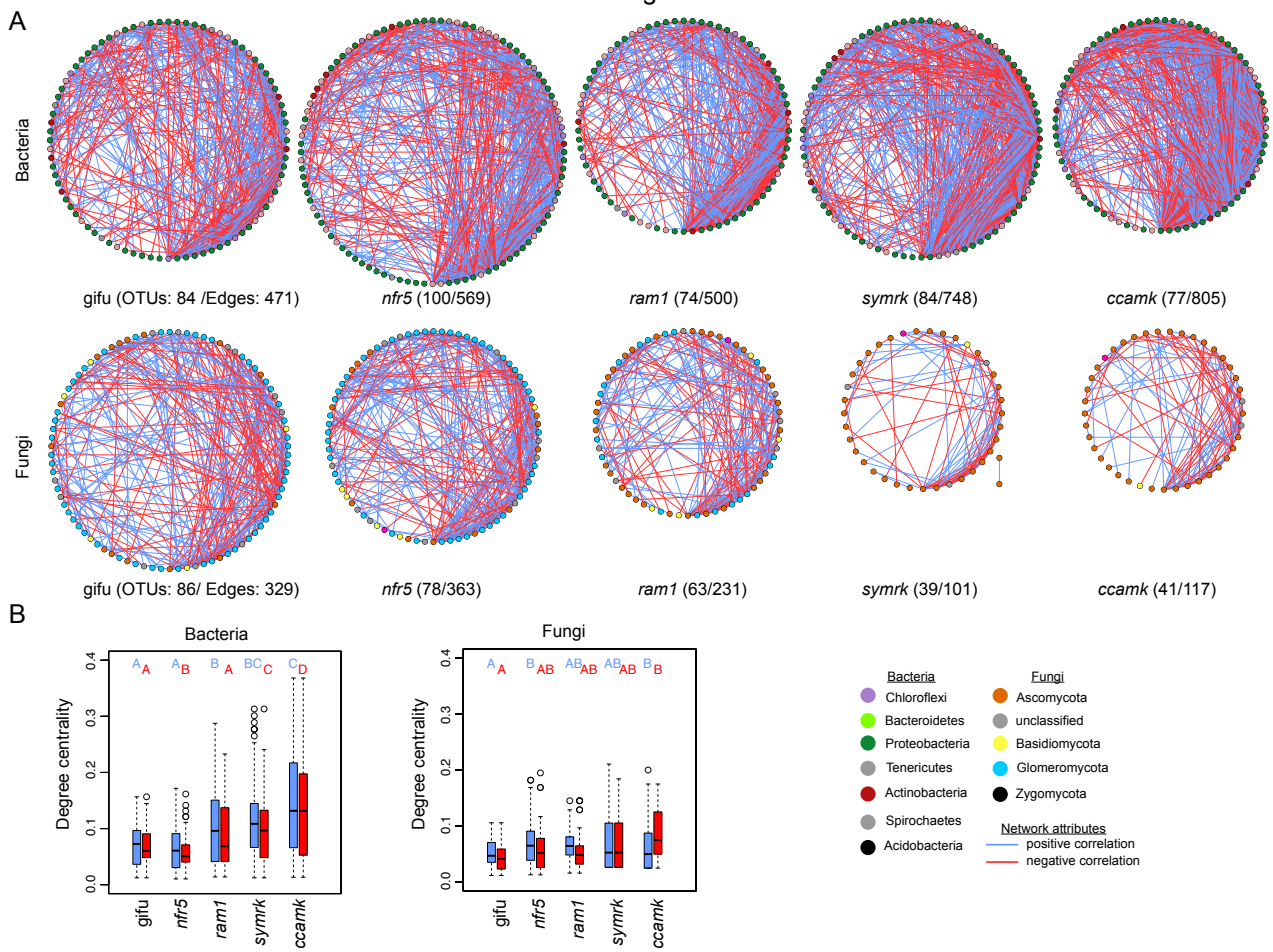

Supp Fig5, Network analysis of root-associated bacterial and fungal OTUs A) SparCC based networks for wildtype and mutant roots (upper panel: bacterial OTUs, lower panel: fungal OTUs). Nodes are colored by phylum and are ordered by increasing degree (clockwise, degree sorted circle layout from Cytoscape). Positive connections are colored in blue, negative connections are colored in red. All connections are significant (SparCC, pseudo p-values $p<0.05$). B) Boxplots showing degree centrality for the different networks. (left panel: bacteria, right panel: fungi). Degree centrality was calculated separately for positive and negative edges, as well as the statistical test were done separate (pairwise Wilcox test, FDR <0.05).

Fig. S6

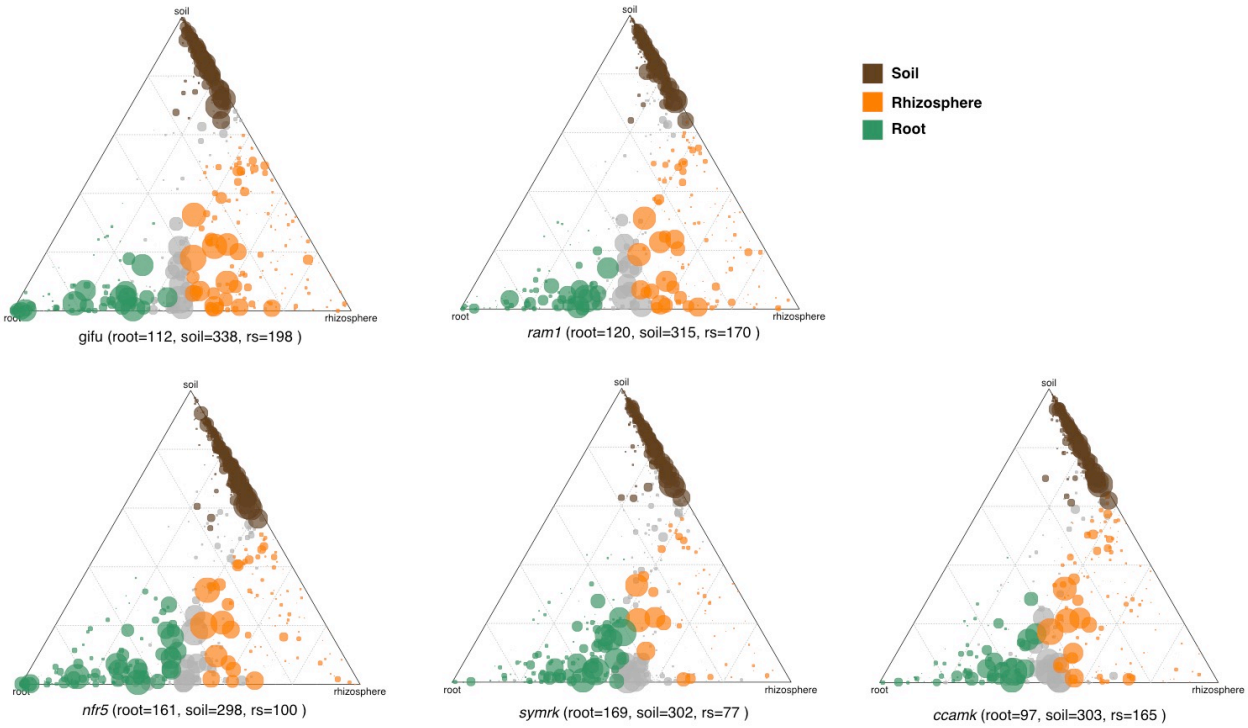

Supp Fig6, Ternary plots showing compartment-enriched bacterial OTUs. Separately for wt and mutant plants. Below each plot the number of enriched OTUs for each compartment is shown.

Fig. S7

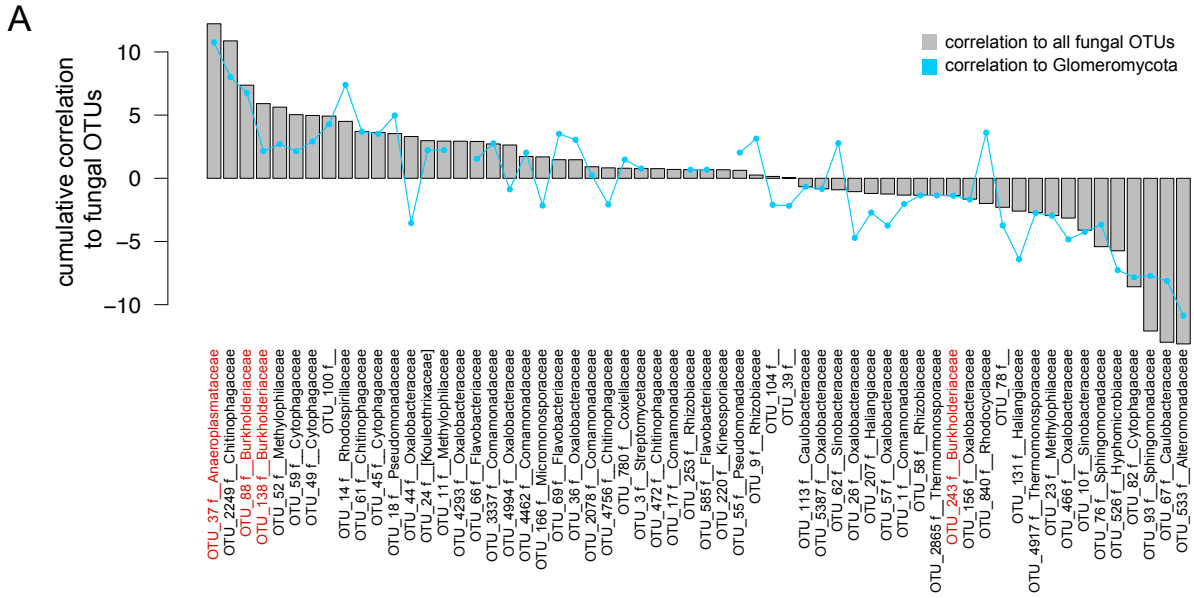

Supp Fig7, Interkingdom correlation of bacterial OTUs in wild-type roots. A) Bacterial OTUs that show a significant correlation to fungal OTUs across wild-type root samples (OTU RA >0.01%, spearman rank correlation p <0.001) are sorted according to their cumulated correlation to all fungal OTUs (grey bars). In addition the cumulative correlation only to Glomeromycotal OTUs is indicated by blue dots within each bar. Taxonomy at the family levels is given for each OTU, if available. OTUs belonging to the Burkholdericeae and Anaeroplasmataceae are highlighted in red.

894 **Supp table1, Symbiotic phenotype of *Lotus japonicus* wild-type and mutants grown in Cologne**
895 **soil** (*n=5*)
896

Genotype	WT(Gifu)	*nfr5-2*	*ram1-2*	*symrk-2*	*ccamk-13*
Colonization (% of root system with intraradical colonisation)	60-70	60-70	10	0	0
Arbuscules	present	present	present	none	none
Nodulation (% of roots with nodules)	100	0	100	0	0

897